

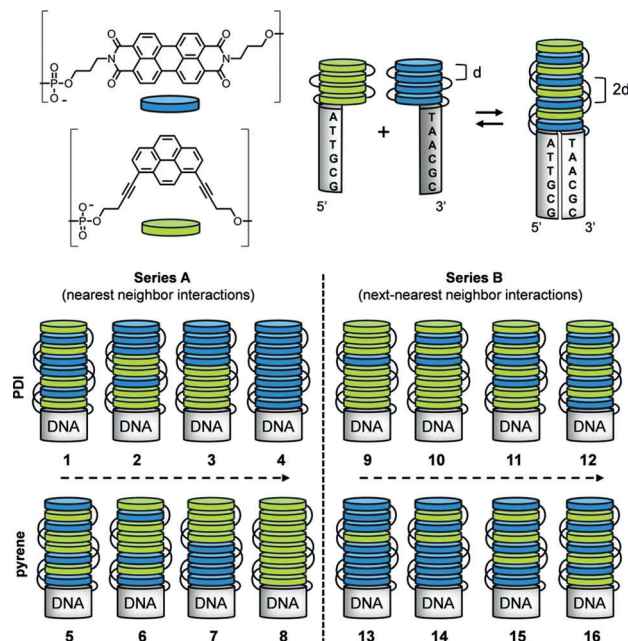
# Formation of Two Homo-chromophoric H-Aggregates in DNA-Assembled Alternating Dye Stacks\*\*

Christian B. Winiger, Simon M. Langenegger, Gion Calzaferri,\* and Robert Häner\*

**Abstract:** The understanding and description of collectively excited multichromophores is of crucial importance for many areas of basic and applied research. DNA has been used for the construction of well-defined heterochromophoric stacks. Electronic coupling among non-adjacent chromophores of the same type leads to the co-existence of PDI and pyrene H-aggregates in hybrids composed of alternating chromophore stacks.

The appearance of collectively excited states of multiple chromophores remains fascinating. More than 70 years after the pioneering contributions of Scheibe,<sup>[1]</sup> Davydov,<sup>[2]</sup> and Kasha,<sup>[3]</sup> the topic has been broadly discussed and reviewed,<sup>[4–9]</sup> but the consequences of collective electronic excitation have by far not been fully explored. For delocalized excitation, a high structural order of the individual chromophores is a prerequisite.<sup>[4,6,10–18]</sup> Yet, the assembly of multichromophores in a precise manner represents a challenge.<sup>[4,19–22]</sup> DNA has been used as a supramolecular scaffold for the construction of distinct arrays of aromatic dyes.<sup>[7,23–33]</sup> The formation of chromophore segments that are well-defined with regard to the number and kind of the components is readily controlled by hybridization of complementary strands. Recently, we reported the DNA-guided assembly of homo- and hetero-multichromophores.<sup>[34]</sup> While this study revealed a correlation between hybrid stability and electrostatic complementarity of the stacked chromophores it also represents a system for testing the degree of electronic coupling among the dye molecules. Herein, we demonstrate the co-existence of excitonic states originating from coupling between identical molecules in alternating chromophore stacks.

The system used for the present study is illustrated in Scheme 1. A total of 14 single strands (Supporting Information) were synthesized according to published procedures.<sup>[34,35]</sup> Oligomers are composed of a short DNA part (six nucleotides) and four consecutive pyrene or perylene-10,9,8,7-tetracarboxylic diimide (PDI) units connected by phosphodiester. Duplexes of



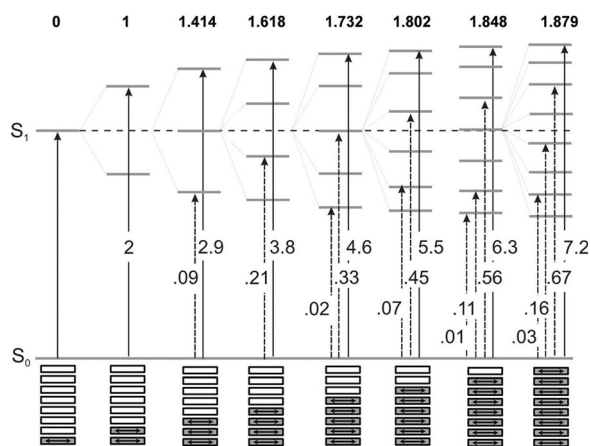
**Scheme 1.** Top: Illustration of PDI (blue) and 1,8-dibutynylpyrene (green) building blocks, modified oligonucleotides, and formation of hybrids 1–16. Bottom: Hybrids grouped in Series A and B (nearest and next-nearest neighbor interactions, increasing in direction of dashed arrows); hybrids shown in the upper panels are used to study electronic coupling among PDIs, interactions of pyrenes are studied with hybrids given in the lower panel.

a specific chromophore composition can be formed by hybridization of two complementary DNA strands. Hybrids 1–8 compose Series A, which allows studying the electronic coupling interactions between nearest neighbors, while hybrids 9–16 (Series B) describe the next-nearest neighbor interactions. PDI and pyrene units in the chromophore segment of the hybrids were previously shown to interact by aromatic stacking interactions.<sup>[34]</sup> Exciton theory is used to describe the electronic coupling in the different hybrids and to explain the co-existence of two independent excitons at different energy levels in the same supramolecular aggregate. In a single chromophore, excitation from  $S_0$  to  $S_1$ <sup>[36]</sup> proceeds by a single transition (Scheme 2). Interaction of  $N$  identical chromophores leads to the splitting of  $S_1$  into  $N$  different energy levels, which are calculated using Equations (1)–(3):  $E_c$  is the reference energy ( $=S_0-S_1$  transition),  $N$  is the number of molecules,  $j$  the numbering of states,  $\beta_c$  is the Coulomb interaction in  $\text{cm}^{-1}$ ,  $AD$  is equal to  $1.615 \times 10^{-18} \text{ m}^2 \text{ cm}^{-1}$ ,  $\bar{\nu}$  is the energy of the  $S_0-S_1$  transition in  $\text{cm}^{-1}$ ,  $n$  is the refractive index (1.40), and  $d$  is the distance between the stacked chromophores (0.35 nm). Scheme 3 illustrates the geometri-

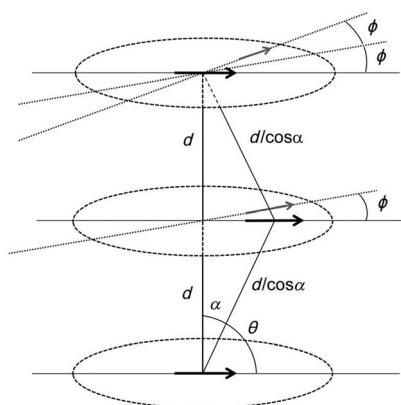
[\*] C. B. Winiger, Dr. S. M. Langenegger, Prof. Dr. G. Calzaferri, Prof. Dr. R. Häner  
Department of Chemistry and Biochemistry, University of Bern  
Freiestrasse 3, 3012 Bern (Switzerland)  
E-mail: gion.calzaferri@dcb.unibe.ch  
robert.haener@dcb.unibe.ch  
Homepage: <http://haener.dcb.unibe.ch>

[\*\*] Financial support by the Swiss National Foundation is gratefully acknowledged (grant 200020\_149148).

Supporting information for this article is available on the WWW under <http://dx.doi.org/10.1002/anie.201410041>.



**Scheme 2.** Representation of the calculated values of the relative exciton interaction and the corresponding ETDMs according to Equations (1)–(4). The uppermost excited state is strongly allowed, whereas the lower states are either forbidden or weakly allowed (for a detailed description and calculated spectra using the obtained values, see the Supporting Information).



**Scheme 3.** Angle representation of stacks of multiple chromophores. The ETDM is represented by the arrows. The angle  $\theta$  arranges the chromophores in either H-aggregates ( $\theta > 54^\circ$ ) or J-aggregates ( $\theta < 54^\circ$ ); for calculations:  $\theta = 90^\circ$ . The angle  $\phi$  defines the self-rotation of the chromophore. The angle  $\phi$  has no substantial influence when  $< 20^\circ$  and is therefore not taken into consideration for further calculations.

cal parameters relevant for the Coulomb interaction between the individual chromophores. The values of the ETDM (electronic transition dipole moment,  $M^2$ ) are further calculated using Equation (4) and are graphically represented in Scheme 2.

$$\varepsilon(j, N) = E_c + 2\beta_c \cos \frac{j}{N+1} \pi \quad (1)$$

$$\beta_c = AD \frac{f k}{\bar{v} d^3 n^2} \quad (2)$$

$$k = \sin^2 \theta \cos \phi - 2 \cos^2 \theta \quad (3)$$

$$M(j) = \mu_a N \sum_{u=1}^N c(j, u) = \mu_a \sqrt{\frac{2}{N+1}} \sum_{u=1}^N \sin \left( j \pi \frac{u}{N+1} \right) \quad (4)$$

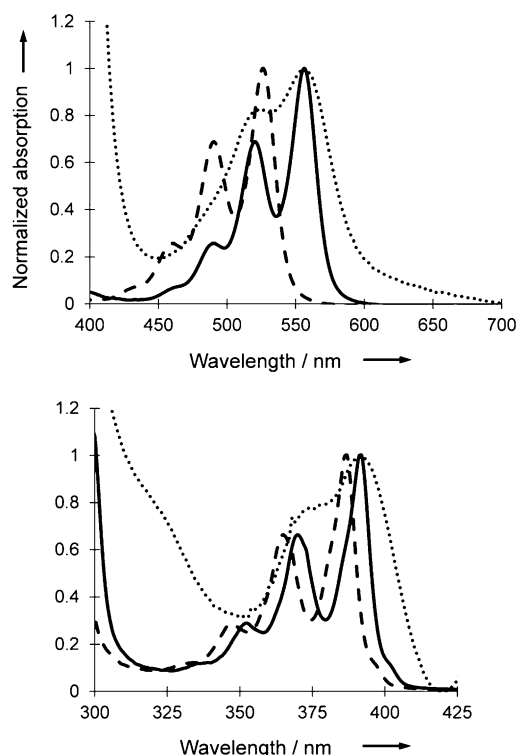


**Figure 1.** Absorption spectra of PDI (top) and pyrene (bottom). Spectra of monomers (----) were shifted by 30 and 5 nm (—), respectively, to match with the actual spectra obtained with duplexes **9** and **13** (••••), which contain a single PDI or pyrene in the chromophore stack. Conditions: 10 mM sodium phosphate buffer, pH 7.2 and 100 mM NaCl; single strand concentration 2.5  $\mu\text{M}$ .

The absorption spectra of duplexes **9** and **13** were used as the pivotal spectra of a single PDI or pyrene building block in a chromophore stack (Figure 1). Both spectra match perfectly (30 and 5 nm shift) with those obtained for the dissolved monomeric compounds (Supporting Information).

In all of the spectra, a certain fraction of monomer contribution is present. Therefore, each calculated spectrum is composed of the spectrum shifted by the amount given in Scheme 2 and fraction of the monomer spectrum (duplex **9**), which was determined individually (for further details, see the Supporting Information). Figure 2 shows the correlation between the calculated and experimental spectra of hybrids **1–4** representing increasing numbers of PDI–PDI nearest neighbor interactions. As seen in Figure 2, the correlation is very good. The only exception is a discrepancy in the 482 nm band in duplex **4**, in which 8 PDIs are in direct contact (for details see the Supporting Information, p 25). The good fit supports H-aggregate interactions between adjacent PDI units. The above calculations and comparison were carried out in an identical way for the duplexes **5–8** in Series A, representing pyrene nearest neighbor interactions. The obtained results were in close agreement with the PDI series (Supporting Information, p 29). For reasons of readability and comprehensiveness, only PDI results are shown here.

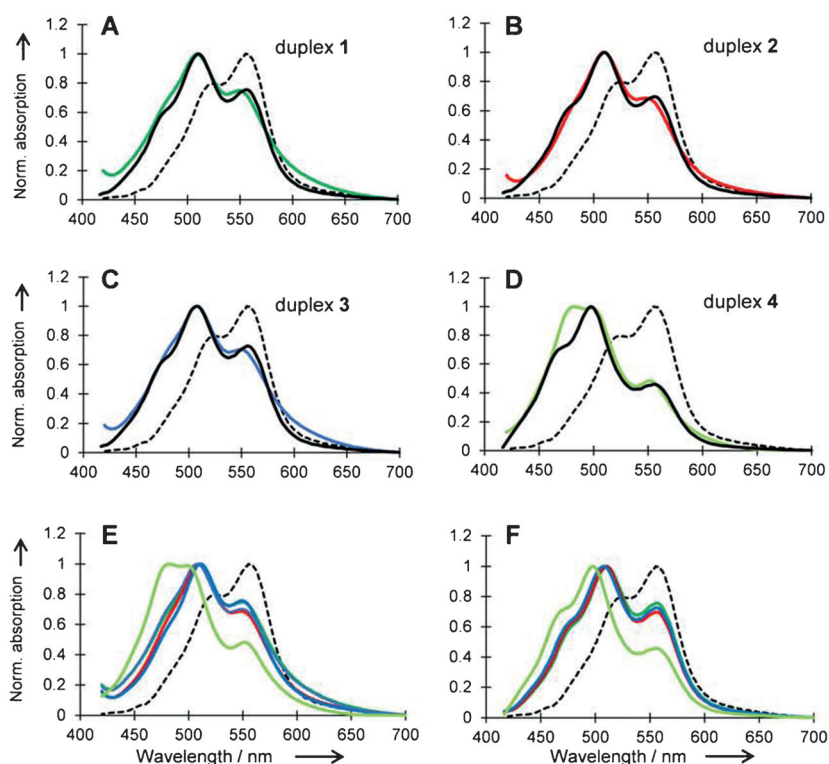


**Figure 2.** Absorption spectra (colored) of duplexes 1–4 showing the effect of an increasing number (A–D: 2, 3, 4, and 8) of adjacent PDIs interacting as nearest neighbors. Black —: calculated spectra; ----: reference spectrum duplex 9 (single PDI). Overlaid spectra (E: observed; F: calculated) are shown at bottom.

Much to our surprise, the same H-coupling behavior can also be observed in Series B containing duplexes in which the PDIs (or pyrenes) can interact exclusively as next-nearest neighbors. The analogous procedure (Supporting Information) was carried out with duplexes 10–12. The correlation

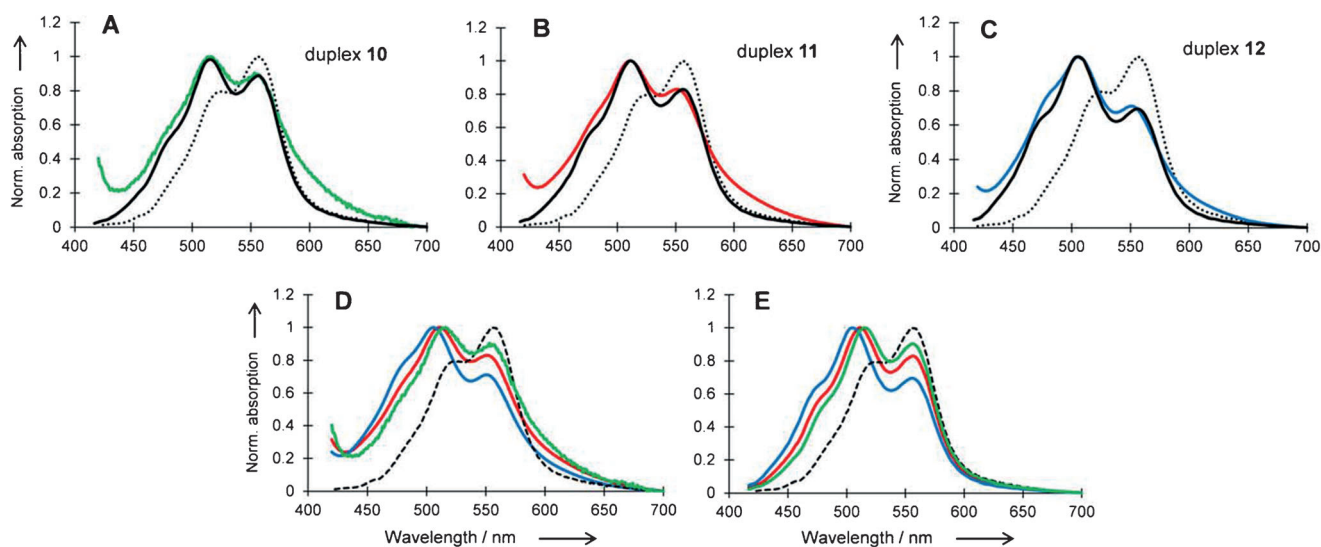


**Figure 3.** Absorption spectra (colored) of duplexes 10–12 showing the effect of an increasing number (A–C: 2, 3, and 4) of PDIs interacting as next-nearest neighbors. Black —: calculated spectra; ----: reference spectrum duplex 9 (single PDI). Overlaid spectra (D: observed; E: calculated) are shown at bottom; conditions as in Figure 2.

between calculated and experimental spectra can be seen in Figure 3. Even though slightly less pronounced than in the nearest neighbor series, a significant blue-shift is observed when two or more PDIs are present in alternating (that is, next-nearest neighbor) positions. Thus, even if they are separated by pyrenes, PDI molecules show strong excitonic coupling. Again, the parallel series (duplexes 14–16) reveals that also pyrenes form H-aggregates by next-nearest neighbor interactions (Supporting Information).

The titration experiment displayed in Figure 4 illustrates the differences between H-aggregates formed from nearest or from next-nearest neighbors. In this experiment, hybrid 16 is formed by the addition of increasing amounts of the pyrene-bearing single strand to the PDI-modified strand. As more and more pyrene component is added, the fraction of single strand (PDI nearest neighbor interactions) decreases while the fraction of duplex (next-nearest neighbor interactions) grows. As a consequence, the relative contribution of the 482 nm band gradually decreases. On the other hand, the relative intensity of the monomer component (550 nm) increases. This transition shows a change from a strong H-coupling owing to nearest neighbor interactions to a less intense H-coupling through next-nearest neighbor interactions.

The data show the existence of an H-aggregate of PDI molecules separated by intervening pyrenes and, vice versa, an H-aggregate of the pyrenes separated by PDIs. The two

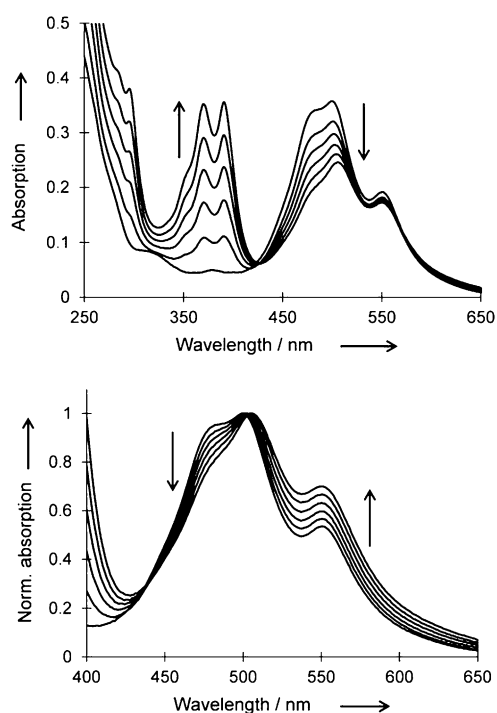
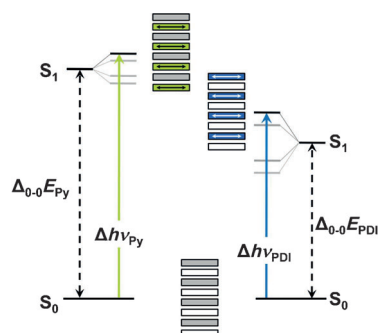


**Figure 4.** Top: Effect of the addition (indicated by arrows, step = 0.2 equiv) of pyrene containing single strand to the PDI-modified strand to form hybrid **16**. Bottom: Normalized absorption traces.



**Scheme 4.** Representation of the two co-existing exciton states (H-aggregates) within an alternating PDI-pyrene stack (pyrene: white/green; PDI: gray/blue).

excitonic states co-exist independently in an aromatic stack composed of alternating PDI and pyrene chromophores. The H-aggregates can be described by classical exciton theory. The co-existence of two separate H-aggregates upon excitation of the two chromophores is illustrated in Scheme 4.

In conclusion, we have demonstrated the co-existence of two independent excitonic states in aromatic stacks composed of two types of chromophores. Pyrene and PDI molecules were arranged in an alternating fashion in a DNA scaffold. Electronic coupling was observed between chromophores of the same type in alternating arrangements. Thus, PDI and pyrene H-aggregates co-exist in  $\pi$ -stacked hetero-aggregates. Classical exciton theory was used to quantitatively explain the data. According to our knowledge this is the first observation

of the co-existence of two independent exciton states in an alternating chromophore stack.

Received: October 13, 2014

Revised: November 18, 2014

Published online: February 3, 2015

**Keywords:** DNA · electronic coupling · H-aggregates · stacking

- [1] G. Scheibe, A. Schöntag, F. Katheder, *Naturwissenschaften* **1939**, 29, 499–501.
- [2] A. S. Davydov, *Usp. Fiz. Nauk* **1964**, 82, 393–448.
- [3] M. Kasha, *Radiat. Res.* **1963**, 20, 55–70.
- [4] J. K. Klosterman, Y. Yamauchi, M. Fujita, *Chem. Soc. Rev.* **2009**, 38, 1714–1725.
- [5] G. Calzaferri, R. Méallet-Renault, D. Brühwiler, R. Pansu, I. Dolamic, T. Dienel, P. Adler, H. R. Li, A. Kunzmann, *Chem-PhysChem* **2011**, 12, 580–594.
- [6] *J-Aggregates* (Ed.: T. Kobayashi), World Scientific Publishing, Singapore, **2012**.
- [7] H. Asanuma, T. Fujii, T. Kato, H. Kashida, *J. Photochem. Photobiol. C* **2012**, 13, 124–135.
- [8] G. D. Scholes, G. Rumbles, *Nat. Mater.* **2006**, 5, 683–696.
- [9] D. Beljonne, C. Curutchet, G. D. Scholes, R. J. Silbey, *J. Phys. Chem. B* **2009**, 113, 6583–6599.
- [10] G. Calzaferri, *Langmuir* **2012**, 28, 6216–6231.
- [11] M. Busby, A. Devaux, C. Blum, V. Subramaniam, G. Calzaferri, L. De Cola, *J. Phys. Chem. C* **2011**, 115, 5974–5988.
- [12] G. Calzaferri, S. Huber, H. Maas, C. Minkowski, *Angew. Chem. Int. Ed.* **2003**, 42, 3732–3758; *Angew. Chem.* **2003**, 115, 3860–3888.
- [13] F. Würthner, T. E. Kaiser, C. R. Saha-Moeller, *Angew. Chem. Int. Ed.* **2011**, 50, 3376–3410; *Angew. Chem.* **2011**, 123, 3436–3473.
- [14] K. C. Hannah, B. A. Armitage, *Acc. Chem. Res.* **2004**, 37, 845–853.
- [15] M. R. Wasielewski, *Acc. Chem. Res.* **2009**, 42, 1910–1921.
- [16] P. P. Neelakandan, T. A. Zeidan, M. McCullagh, G. C. Schatz, J. Vura-Weis, C. H. Kim, M. R. Wasielewski, F. D. Lewis, *Chem. Sci.* **2014**, 5, 973–981.
- [17] K. Rao, V. K. Datta, M. Eswaramoorthy, S. J. George, *Chem. Eur. J.* **2012**, 18, 2184–2194.
- [18] M. Vybornyi, A. V. Rudnev, S. M. Langenegger, T. Wandlowski, G. Calzaferri, R. Häner, *Angew. Chem. Int. Ed.* **2013**, 52, 11488–11493; *Angew. Chem.* **2013**, 125, 11702–11707.
- [19] A. Wilson, G. Gasparini, S. Matile, *Chem. Soc. Rev.* **2014**, 43, 1948–1962.
- [20] G. J. Gabriel, B. L. Iverson, *J. Am. Chem. Soc.* **2002**, 124, 15174–15175.
- [21] F. C. De Schryver, T. Vosch, M. Cotlet, M. Van der Auweraer, K. Müllen, J. Hofkens, *Acc. Chem. Res.* **2005**, 38, 514–522.
- [22] S. Ghosh, X. Q. Li, V. Stepanenko, F. Würthner, *Chem. Eur. J.* **2008**, 14, 11343–11357.
- [23] V. V. Filichev, E. B. Pedersen, *Wiley Encycl. Chem. Biol.* **2009**, 1, 493–524.
- [24] R. Varghese, H. A. Wagenknecht, *Chem. Commun.* **2009**, 2615–2624.
- [25] V. L. Malinovskii, D. Wenger, R. Häner, *Chem. Soc. Rev.* **2010**, 39, 410–422.
- [26] M. E. Østergaard, P. J. Hrdlicka, *Chem. Soc. Rev.* **2011**, 40, 5771–5788.
- [27] E. Stulz, *Chem. Eur. J.* **2012**, 18, 4456–4469.
- [28] Y. N. Teo, E. T. Kool, *Chem. Rev.* **2012**, 112, 4221–4245.
- [29] H. Kashida, H. Asanuma, M. Komiya, *Angew. Chem. Int. Ed.* **2004**, 43, 6522–6525; *Angew. Chem.* **2004**, 116, 6684–6687.



- [30] I. K. Astakhova, J. Wengel, *Acc. Chem. Res.* **2014**, *47*, 1768–1777.
- [31] T. Takada, Y. Kawano, A. Ashida, M. Nakamura, K. Kawai, T. Majima, K. Yamana, *Tetrahedron Lett.* **2013**, *54*, 4796–4799.
- [32] F. D. Lewis, L. G. Zhang, X. Y. Liu, X. B. Zuo, D. M. Tiede, H. Long, G. C. Schatz, *J. Am. Chem. Soc.* **2005**, *127*, 14445–14453.
- [33] T. S. Kumar, A. S. Madsen, M. E. Ostergaard, J. Wengel, P. J. Hrdlicka, *J. Org. Chem.* **2008**, *73*, 7060–7066.
- [34] C. B. Winiger, S. M. Langenegger, O. Khorev, R. Häner, *Beilstein J. Org. Chem.* **2014**, *10*, 1589–1595.
- [35] S. M. Biner, D. Kummer, V. L. Malinovskii, R. Häner, *Org. Biomol. Chem.* **2011**, *9*, 2628–2633.
- [36] In contrast to unsubstituted pyrene, for which the  $S_0-S_1$  transition is symmetry-forbidden, this transition is allowed in 1-substituted pyrenes; see for example: A. G. Crawford, A. D. Dwyer, Z. Liu, A. Steffen, A. Beeby, L. O. Palsson, D. J. Tozer, T. B. Marder, *J. Am. Chem. Soc.* **2011**, *133*, 13349–13362.
-